NASA Technical Memorandum 81478

RADIATION DAMAGE IN HIGH VOLTAGE SILICON SOLAR CELLS

Irving Weinberg, Henry W. Brandhorst, Jr.,
Clifford K. Swartz, and Victor G. Weizer
Lewis Research Center
Cleveland, Ohio

Prepared for the
Second European Symposium on Photovoltaic
Generators in Space
Heidelberg, Germany, April 15-17, 1980

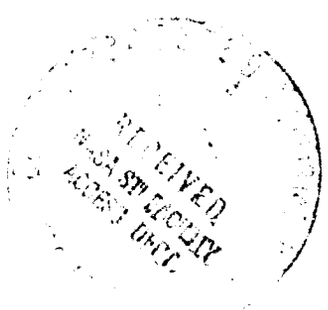

RADIATION DAMAGE IN HIGH VOLTAGE SILICON SOLAR CELLS

by Irving Weinberg, Henry W. Brandhorst, Jr., Clifford K. Swartz, and Victor G. Weizer

NASA Lewis Research Center
Cleveland, Ohio

E-412

ABSTRACT

Three high open-circuit voltage cell designs based on 0.1 ohm-cm p-type silicon were irradiated with 1 MeV electrons and their performance determined to fluences as high as $10^{15}/cm^2$. Of the three cell designs, radiation induced degradation was greatest in the high-low emitter (HLE cell. The diffused and ion implanted cells degraded approximately equally but less than the HLE cell. Degradation was greatest in an HLE Cell exposed to X-rays before electron irradiation. The cell regions controlling both short-circuit current and open-circuit voltag degradation were defined in all three cell types. An increase in front surface recombination velocity accompanied time dependent degradation of an HLE cell after X-irradiation. It was speculated that this was indirectly due to a decrease in positive charge at the silicon-oxide interface. Modifications aimed at reducing radiation induced degradation are proposed for all three cell types.

Keywords

Radiation damage, High V_{oc}, Electron irradiation, X-rays, Surface recombination, Time dependent degration, Oxide charge

1. INTRODUCTION

It has been predicted that n^+/p silicon solar cells with low p-base resistivities (≈0.1 ohm-cm,) could achieve air mass zero (AMO) efficiencies as high as 19% if, among other things, open-circuit voltages (V_{oc}) of 700 mV could be attained (ref. 1). Hence, as a first step toward achievement of the higher efficiency goal, the NASA Lewis Research Center initiated a program aimed at demonstrating that significant increases in V_{oc} could be achieved in 0.1 ohm-cm cells. To date three cell designs have been developed under this program and open-circuit voltages of 645 millivolts have been achieved. Although the program was directed toward demonstrating increased V_{oc}, the degrading effects of the particulate space radiation environment were of equal concern. Hence in the present work we present the results of our determination of cell performance after 1 MeV electron irradiation. In addition we present calculations and experimental data to define the cell regions controlling short-circuit current (I_{sc}), and V_{oc} degradation in all three cell types. These results are used as a basis for suggested cell modifications directed toward reducing the radiation induced degradation.

2. EXPERIMENTAL PROCEDURES

The salient features of the cells are given in Table I. The ion-implanted (ref. 2) and high-low emitter (HLE) (ref. 3) cells have thermally grown silicon dioxide (SiO_2) on their front surfaces; the diffused cells (ref. 4) have no front-surface oxide. The oxide on the HLE cells was formed by using a temperature-time schedule that results in a net positive charge, in the oxide, near the oxide-silicon interface (ref. 5). The positive oxide charge induces an accumulation layer at the silicon surface and thus establishes an n^+n high-low emitter junction.

Pre-irradiation AMO parameters, obtained using a Xenon-arc solar simulator at 25° C are shown in Table II. In addition to the data shown in Table II, spectral response and diffusion length measurements were made. The spectral response data were obtained by using a filter-wheel spectral response apparatus (ref. 6). The diffusion length data were obtained by an X-ray excitation technique using 250 keV X-rays (ref. 7). both X- and electron irradiation can cause changes in oxide charge (refs. 8 & 9), therefore, only one of each pair of oxide coated cells was exposed to X-irradiation. However, all cells were exposed to 1 MeV electron irradiation to a maximum fluence of 10^{15} cm^{-2}.

3. RESULTS

A typical data plot used in the process of determining the diffusion length damage coefficient, K_L, is shown in Fig. 1. The damage coefficients were calculated from the relation;

$$\frac{1}{L^2} - \frac{1}{L_o^2} = K_L \phi \qquad (1)$$

where L is diffusion length after irradiation at the fluence ϕ and L_o is diffusion length before irradiation. Table III summarizes the damage coefficients obtained for each cell design. Comparison with previous damage coefficient evaluations (ref. 10) indicates that the damage coefficients obtained for the present cells are typical of 0.1 ohm-cm silicon.

Plots of normalized short-circuit current, I_{sc}, and open-circuit voltage, V_{oc}, as a function of 1 MeV electron fluence are shown in figures 2 and 3 respectively. Data for a 10 ohm-cm cell are included for comparison. This cell showed a decrease in output typical of 10 ohm-cm resitivity. In general, performance degradation under irradiation was highest for the HLE cells, with greatest degradation being noted for the X-rayed HLE cell. For the ion-implanted cells, there was no measurable difference between the X-rayed and non-X-rayed cell performance. Both diffused and ion-implanted cell designs degraded at a rate typical of conventional 0.1 ohm-cm cells. The higher I_{sc} and V_{oc} degradation data for the HLE cells appears to be anomalous because K_L is approximately the same for all cell designs. As an aid in clarifying the sources of I_{sc} degradation, the normalized data for long and short-wavelength spectral response were plotted as shown in figures 4 and 5. Further discussion of these data and the degradation in V_{oc} are contained in the next section.

4. ANALYSIS AND DISCUSSION

In assessing radiation damage effects it is significant to know the cell regions responsible for loss of cell performance. This information is needed to guide future work aimed at increasing the radiation resistance of these high V_{oc} cells. for this reason we first focus our attention on determination of the cell regions in which current and voltage degradation occur.

4.1 Cell Regions Controlling I_{sc}

The sources of I_{sc} degradation are clarified by examination of the short and long wavelength spectral response of figures 4 and 5. Noting that substantial I_{sc} degradation for the HLE cells occurs at both long-and short wavelengths we conclude that I_{sc} of the cell is controlled by both the p-type base and n-type emitter. On the other hand, I_{sc} degradation of the ion imiplanted and diffused cells occurs predominantly at long wavelengths and therefore I_{sc} is controlled predominantly by the p-type base region. This tends to explain the relatively higher I_{sc} degradation observed in the HLE cells despite the approximate equality of K_L for all cell designs. The diffusion length damage coefficient applies to the base regions of the solar cell while the spectral response data indicate that, for the HLE cells, both base and emitter region must be considered as factors in current degradation.

4.2 Cell Regions Controlling V_{oc}

4.2.1 Diffused Cell. The open-circuit voltage of this cell can be expressed as a function of I_{oE} and I_{oB}, the emitter and base device saturation currents, i.e.

$$V_{oc} = \frac{kT}{q} \ln\left\{\frac{I_{sc}}{I_{oB} + I_{oE}}\right\} \qquad (2a)$$

where (ref. 11);

$$I_{oE} = \frac{qn_i^2 D_E}{N_E L_E}\left\{\frac{\frac{S_F L_E}{D_E} + \tanh\frac{W_E}{L_E}}{1 + \frac{S_F L_E}{D_E}\tanh\frac{W_E}{L_E}}\right\} \qquad (2b)$$

$$I_{oB} = \frac{A}{L_B}\coth\frac{W_B}{L_B} \qquad (2c)$$

$$A = \frac{qn_i^2 D_B}{N_B}$$

where W is region thickness, L is minority carrier diffusion length S_F is front surface recombination velocity, N is the doping concentration, D is minority carrier diffusivity, n_i is the intrinsic carrier concentration, q is the electronic charge, T is the temperature in degress Kelvin, k is Boltzmann's constant, the subscripts E and B refer to the emitter and base respectively, and an ohmic base contact is assumed. Equation (2) can be simplified by considering the data of figure 4 and 5. As can be seen from the figures, for the diffused cell, the long wavelength response is severely degraded by the irradiation but the short wavelength response is relatively unaffected. We therefore assume, in the following, discussion that this relative invariance of the short wavelength response with fluence indicates that I_{oE} is unaffected by the irradiation. We can thus treat I_{oE} as a constant to be determined by fitting equation (2) to the measured V_{oc} vs L_B data shown in figure 6. A fit of equation (2a) to the data, using I_{oE} and A as adjustable parameters and calculating I_{oB} from (2c) is shown as the solid curve in that figure. The result of the fit indicates that the voltage of the cell is controlled by the base component of the saturation current. Before irradiaton, the base component contributes 68% of the saturation current, while the emitter component contributes only 32%. As the cell is irradiated, the base diffusion length decreases thus increasing I_{oB} and decreasing V_{oc}. For these cells, the drop in voltage with fluence is caused by events occurring in the base. The drop is not as severe, however, as it would be were the cell 100% base controlled.

4.2.2 Ion Implanted Cells. Because the ion-implanted cells also exhibit a relative invariance of short wavelength response with fluence (fig. 4), we performed an analysis similar to that for the diffused cell. The results indicate that the voltage in this type of cell is also controlled by its base parameters. Our calculations show that the pre-irradiation device saturation current is composed of a 39% contribution from the emitter. These data indicate that, as the cell is irradiated, the voltage is controlled by changes in the base parameters. Again, however, a more severe drop would be expected had the pre-irradiated cell been fully base controlled.

4.2.3 HLE Cell. Since both short and long wavelength components of the HLE cell were found to be degraded by electron irradiation, an assumption of constant I_{oE} cannot be made. While a quantitative analysis of radiation induced degradation is

difficult, qualitative conclusions can be drawn, using equations (2a, 2b, and 2c). Figure 7 shows the experimental change of V_{oc} with fluence for the HLE cell. Superimposed on these data is a curve illustrating what would be expected if the voltage of the cell were controlled only by the measured radiation induced decrease in the base diffusion length L_B. As can be seen, the base component can account for only a small fraction of the observed voltage drop. We thus conclude that V_{oc} in the HLE cell is controlled to a high degree by the emitter component of the device saturation current.

It can also be concluded that the voltage reduction in these cells at high fluence is due to degradation of bulk parameters and not to surface effects. this follows from results of attempts to model the voltage decrease with fluence by manipulating both surface and bulk parameters. Calculations indicate that at high fluence levels, e ter diffusion lengths much less than the emitter thickness are required to explain the data. When $L_E << W_E$ the surface is electrically isolated from the junction and thus would have no effect on the voltage. The degradation at low fluences may be controlled by a combination of bulk and surface phenomena, but the voltage at the $10^{14} e/cm^2$ level appears to be controlled only by the emitter diffusion length.

4.3 Effects of X-rays

In establishing the cell regions which control cell degradation, the preceding calculations do not consider possible degradation in the charged oxide of the HLE cell. In view of ite anomalously large degradation in I_{sc}, observed for the X-rayed HLE cell, consideration needs to be given to possible oxide degradation due to X-rays alone. In this connection, it has been established that ionizing radiation affects the charge state of SiO_2 in MOS devices (refs. 8 & 9). Hence, so that the effects of X-rays on the HLE charged-oxide cells could be explored, an additional HLE cell was exposed to the 250 KeV X-rays for 5 minutes and its performance parameters determined for times up to 93 days after X-irradiation. Variation in spectral response with time is shown in figure 8 while variation in I_{sc} and V_{oc} are shown in figure 9. From the latter figure it is seen that significant variations in I_{sc} and V_{oc} are observed as a function of time after X-irradiation.

The spectral response data (fig. 8) indicates that, as a result of X-irradiation, the major change occurs at short wavelengths and hence in the emitter of the HLE cell. One possible source of emitter degradation is a decrease in the magnitude of the induced front surface accumulation layer. This would also result in increased front surface recombination velocity with accompanying degradation in cell performance. To ascertain whether this could be the case, we have calculated S_F as a function of time using equations (2a, 2b, and 2c) and the data of figure 9. In evaluating S_F it is assumed that L_E and L_B are constant with time. Using the measured value for L_B of about 50 μm, a pre-irradiation value for S_F of 10^3 cm/sec and a value for L_E of 24.9 μm as calculated from equations (2a, 2b, and 2c), we obtain the time dependent values of S_F shown in figure 10. The increase in S_F by itself is not sufficient to account for the loss in response. It is also necessary to include reduction in the magnitude of the induced front surface accumulation layer to explain the data. Thus, it appears that as S_F increases, there is a concomitant decrease in negative charge in the accumulation layer which constitutes the n^+ region in the n^+n high-low emitter junction. This in turn implies a decrease in the positive oxide charge at the silicon-oxide interface as a result of X-irradiation. The mechanism by which this hypothesized charge reduction could occur is unclear at present. We should note that it is possible that the total positive charge in the oxide could be increasing with X-ray fluence. An alternate explanation lies in a time dependent decrease in L_E. However, since the X-rays alone do not damage the silicon it is reasonable to assume a constant L_E during a after X-irradiation.

The I_{sc} degradation of figure 9 is insufficient to account for the difference in total short-circuit current degradation between the X-rayed and none X-rayed HLE cells after electron irradiation (fig. 2). One source of the added I_{sc} degradation could be synergism between the effects of X- and electron-irradiation. Another possible source of the added degradation could be a difference in quality of the silicon contituting the emitters and bases of the two HLE cells.

4.4 Recommended Cell Modification

From the preceding results it is clear that for increased radiation resistance in the diffused and ion-implanted cells, improvement in the base region are required while for the HLE cell, modifications are required in both the emitter and base regions of the solar cell.

For the diffused and ion-implanted cells, the base region could be improved by treatments which remove lattice strain and the use of cell processing which tends to decrease impurity concentrations in the base. The impurities in question are those which form radiation induced complexes capable of decreaseing L_B. Similar requirements apply to the base and emitter of the HLE cell.

For the HLE cells, one source of the increased degradation is the use of a relatively deep (10 μm) n-type emitter. The damage coefficient for n-type silicon is about an order of magnitude greater than that for p-type silicon (ref. 12). Because about 75 percent of the incoming optical radiation is absorbed in the 10-micrometer wide HLE n-region, the increased susceptibility of n-type silicon to radiation damage is reflected in the large loss in blue spectral response which would be expected and was observed. Thus, one modification to the HLE cell would be use of a shallower n-type emitter.

With regard to the use of a charged oxide in the HLE cell, it is not clear at present whether this contributes to decreased radiation resistance of the HLE cell. The data of figures 2, 8, 9, and 10 and the accompanying analysis suggest that oxide charge is reduced by the ionizing radiation. However, additional work is necessary to verify this typothesis. It is noted that the sole function of the oxide charge is to induce an accumulation layer, thus forming the n^+n junction at the emitter surface. The n^+n junction could be formed by other means such as ion-implantation, without the necessity for oxide charge. This should be done and the resultant cells radiation resistance compared to those in which oxide charge plays a key role.

5. SUMMARY

The results of this work are summarized as follows:

1. Of the high V_{oc} cells investigated under 1 MeV electron bombardment, degradation is greatest in the HLE cell ard least in the diffused and ion-implanted cells, degradation being equal in the latter two cell types. The greetest degration was noted for an HLE cell subjected to X-rays prior to electron irradiation.

2. The cell regions controlling I_{sc} and V_{oc} degradation were defined. For the HLE cells both emitter and base control I_{sc} while for the diffused and ion-implanted cells I_{sc} is base controleed. The V_{oc} is emitter controlled in the HLE cell and base controlled in the ion-implanted and diffused cells.

3. After X-irradiation alone, time dependent decays in I_{sc} and V_{oc} were observed in the HLE cell. We speculate that these can be explained by increases in front surface recombination velocity which was indirectly related to a decrease in positive oxide charge near the oxide-silicon interface.

4. For increased radiation resistance, decreased processing induced defect concentrations are required in the base region of all 3 cell types and in the emitter region of the HLE cell. In addition, for the HLE cell, it is recommended that the 10 μm emitter width be decreased and consideration be given to alternate means, other than oxide charge, to achieve the n^+n high-low emitter junction.

REFERENCES

1. Godlewski M P et al 1975, Effects of High Doping Levels on Silicon Solar Cell Performance, 11th IEEE Photovoltaic Specialists Conference, Phoenix 6-8 May 1975, 32-35.

2. MR-10056-07 (Spire Corp) 1979, Study Program to Improve the Open-circuit Voltage of Low Resistivity Single Crystal Silicon Solar Cells, by Minnucci J.

3. NASA Grant NSG 3018, Final Report, 1979, Studies of Silicon PN Junction Solar Cells, by Neugroschel A & Lindholm F A.

4. The diffused cell was fabricated in-house at the NASA Lewis Research Center.

5. Sah C T et al 1972, The Scattering of Electrons by Surface Oxide Charges and by Lattice Vibrations at the Silicon-Silicon Dioxide Interface, Surface Sci 32, 561-575.

6. NASA TN D-2562, 1965, Filter-Wheel Solar Simulator, by Mandelkorn J et al.

7. Rosenzwieg W 1962, Diffusion Length Measurement by Means of Ionizing Radiation, Bell Sys Tech J 41 5, 1573-1588.

8. Collins D R & Sah C T 1966, Effects of X-Ray Irradiation on the Characteristics of Metal-Oxide-Silicon Structures. Appl Phys Lett 8, 5, 124-126.

9. Zaininger K H 1966, Electron Bombardment of MOS capacitors, Appl Phys Lett 8, 6, 140-142.

10. NRTC-75-23R (NASA-CR-134768) 1975, Damage Coefficients in Low Resistivity Silicon, by Srour J R et al.

11. McKelvey J P 1966, Solid State and Semiconductor Physics, New York, Harper & Row.

12. PIC-SOL-209/5 (NASA-CR-58680) 1964, The Energy Dependence of Electron Damage in Silicon, Proceedings of the Fourth Photovoltaic Specialists Conference, Vol. 1, A-5-1 to A-5-33, by Downing R G.

TABLE I-FEATURES OF HIGH V_{oc} CELLS

Cell Property	Cell Type		
	Ion-Implanted	Hi-lo emitter	Diffused
Oxide	SiO_2 (0.1 μm)	SiO_2 (0.1 μm) (+ Charge near Interface)	None
N-Layer depth, microns	0.2-0.3	10	1.5-2
Cell thickness, microns	300	260	200

Base resistivity 0.1 OHM-CM
All cells n on p

TABLE II PREIRRADIATION AMO CELL PARAMETERS

	V_{oc} mV	I_{sc}, mA/cm²	P_{max}, mW/cm²	FF, %	X-Irradiated Yes	X-Irradiated No
Ion Implanted	636	34.4	14.4	65.8		X
	636	35.5	14.5	64.1	X	
Diffused	626	20.3	9.3	73.3	X	
	623	19.8	9.2	74.4	X	
HLE	634	31.2	13.5	68		X
	640	28.6	14	76.5	X	

TABLE III-DIFFUSION LENGTH DAMAGE COEFFICIENTS
(a) Present data

Cell Type	Diffusion-Length damage-coefficient K_L
Ion implanted	8×10^{-10}
Diffused	9×10^{-10}
HLE	10×10^{-10}

(b) Previous data - 0.1 ohm-cm cells

Research	Diffusion-Length damage coefficient K_L
Srour, et al (ref. 10) 1974	7×10^{-10} to 8×10^{-10}
Lewis data (unpublished) 1973	9×10^{-10}

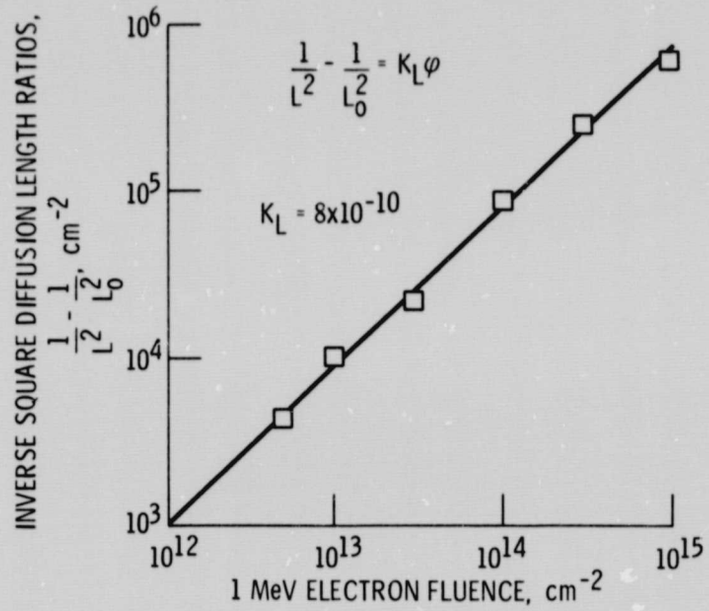

Figure 1. - Determination of diffusion length damage coefficient for high voltage cell.

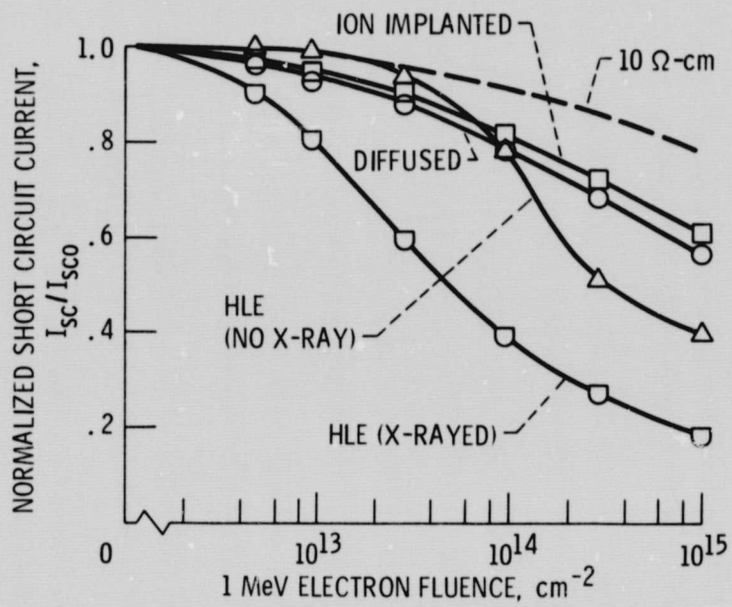

Figure 2. - Change in normalized short circuit current with 1 MeV electron fluence.

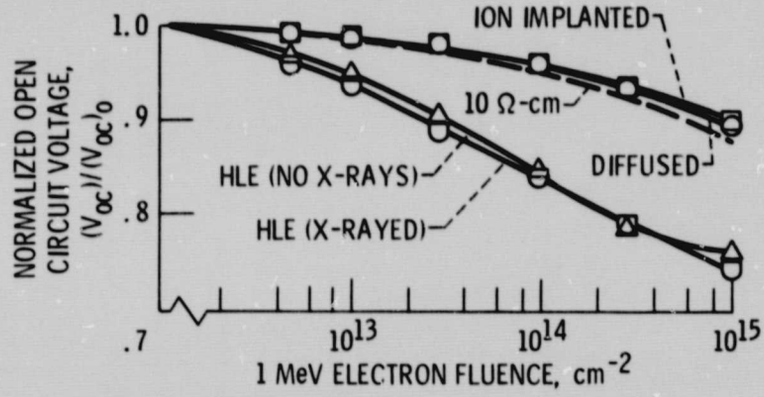

Figure 3. - Change in normalized open circuit voltage with 1 MeV electron fluence.

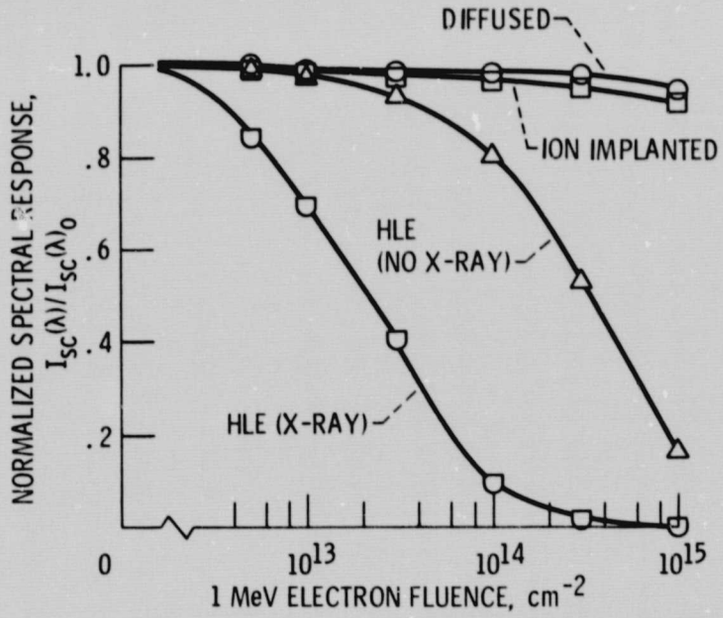

Figure 4. - Variation of normalized 0.45 micrometer spectral response after irradiation with 1 MeV electrons.

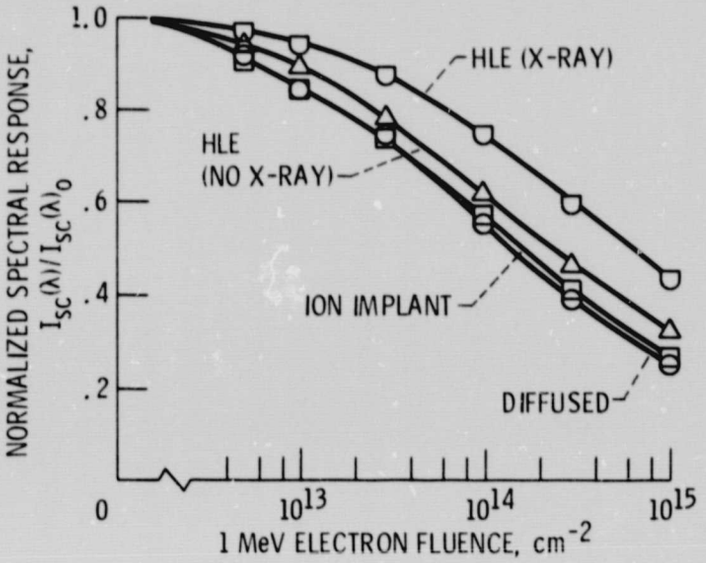

Figure 5. - Variation of normalized 0.9 micrometer spectral response after irradiation with 1 MeV electrons.

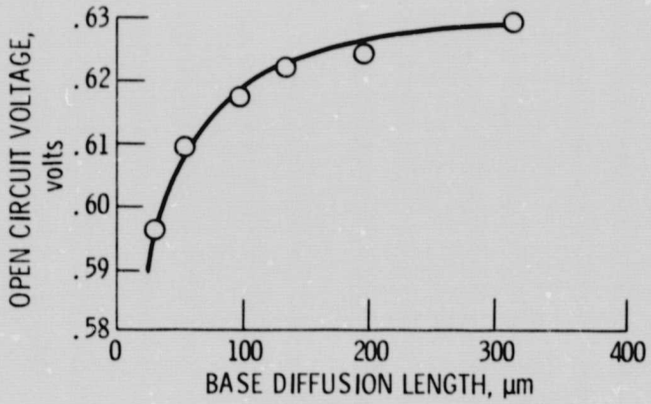

Figure 6. - Influence of base diffusion length on open circuit voltage for diffused cell.

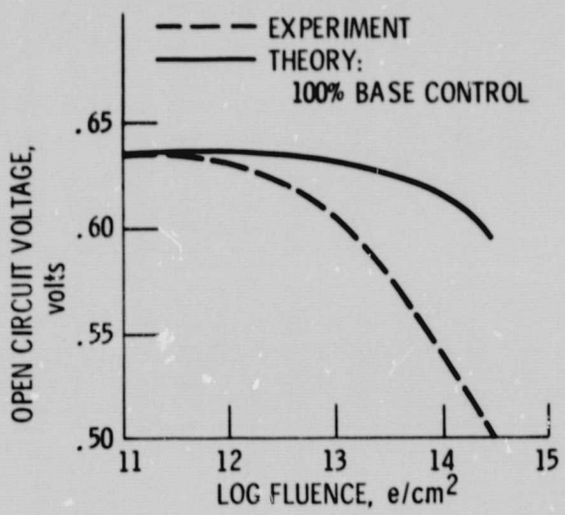

Figure 7. - Change in V_{oc} with fluence for HLE cell.

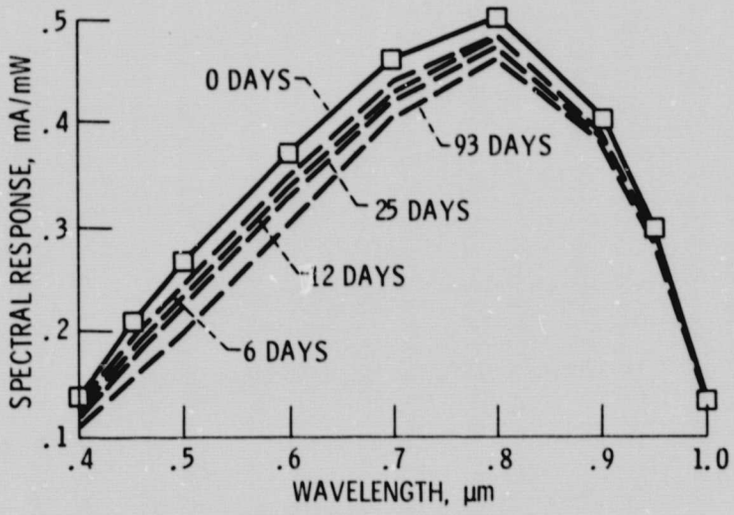

Figure 8. - Spectral response of HLE cell after X-irradiation alone.

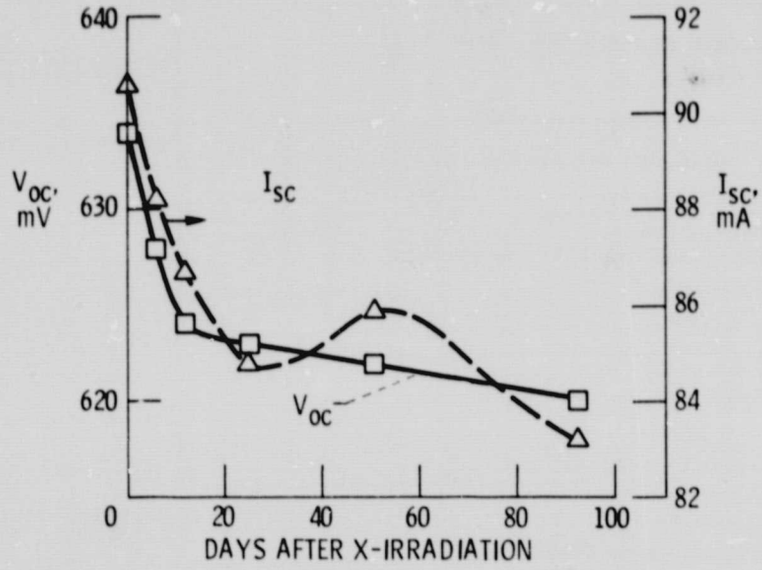

Figure 9. - Decay in I_{sc} and V_{oc} of HLE cell after X-irradiation alone.

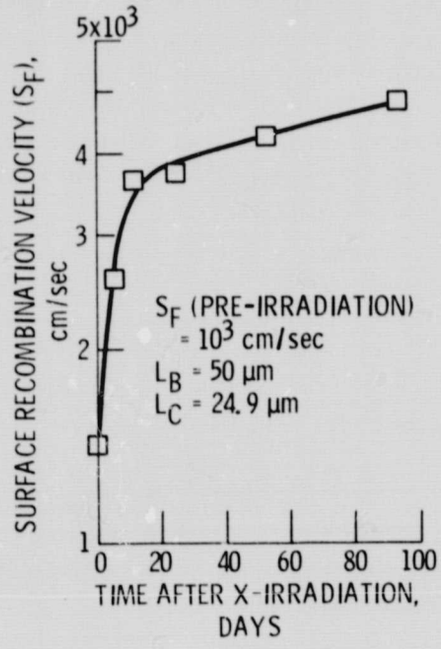

Figure 10. - Surface recombination velocity after X-irradiation (HLE cell).